

Fronto-Thalamic Structural Connectivity Associated With Schizotypy, a Psychosis Risk Phenotype, in Nonclinical Subjects

Igor Nenadić^{1,2,*}, Johannes Mosebach¹, Simon Schmitt^{1,2,3}, Tina Meller^{1,2}, Frederike Stein^{1,2}, Katharina Brosch^{1,2}, Kai Ringwald^{1,2}, Julia-Katharina Pfarr^{1,2}, Susanne Meinert^{4,5}, Hannah Lemke⁴, Lena Waltemate⁴, Katharina Thiel⁴, Nils Opel^{4,6,7}, Jonathan Repple^{4,8}, Dominik Grotegerd⁴, Olaf Steinsträter^{1,2,9}, Jens Sommer^{1,2,9}, Tim Hahn⁴, Andreas Jansen^{1,2,9}, Udo Dannlowski⁴, Axel Krug^{1,2,10}, and Tilo Kircher^{1,2}

¹Department of Psychiatry and Psychotherapy, Philipps-Universität Marburg, Marburg, Germany; ²Center for Mind, Brain and Behavior (CMBB), Marburg, Germany; ³Present address: Department of Psychiatry and Psychotherapy, MH Hannover, Hannover, Germany; ⁴Institute for Translational Psychiatry, University of Münster, Münster, Germany; ⁵Institute for Translational Neuroscience, University of Münster, Germany; ⁶Department of Psychiatry and Psychotherapy, University Hospital Jena, Jena, Germany; ⁷German Center for Mental Health (DZPG), Jena, Germany; ⁸Department of Psychiatry, Psychosomatic Medicine and Psychotherapy, Goethe University Frankfurt, University Hospital, Frankfurt, Germany; ⁹Core-Facility BrainImaging, School of Medicine, Philipps-Universität Marburg, Marburg, Germany; ¹⁰Department of Psychiatry and Psychotherapy, University Hospital Bonn, Bonn, Germany

*To whom correspondence should be addressed; Department of Psychiatry and Psychotherapy, Philipps University of Marburg, Rudolf-Bultmann-Str. 8, 35039 Marburg, Germany; tel: +49 6421 58 65002, fax: +49 6421 58 68939, email: nenadic@staff.uni-marburg.de

Background and Hypothesis: Schizotypy is a risk phenotype for the psychosis spectrum and pilot studies suggest a biological continuum underlying this phenotype across health and disease. It is unclear whether this biological continuum might include brain structural associations in networks altered in schizophrenia spectrum disorders, such as the fronto-thalamo-striatal system or nodes of the default mode network, such as the precuneus. **Study Design:** In this study, we analyze a large multi-center cohort of 673 non-clinical subjects phenotyped for schizotypal traits (using the Schizotypal Personality Questionnaire-Brief version) using tract-based spatial statistics of diffusion tensor imaging data, as well as voxel-based morphometry (VBM) analysis of regional brain volumes and gyrification analysis of early neurodevelopmental markers of cortical folding on T1-weighted MRI. **Study Results:** We identify significant ($P < .05$ family-wise error corrected) associations of schizotypy with major fiber tract fractional anisotropy: positive (cognitive-perceptual) schizotypy correlated negatively with the left anterior thalamic radiation (a principal thalamo-frontal projection), left uncinate fasciculus and cingulum, while negative (interpersonal) schizotypy correlated positively with left anterior thalamic radiation, cingulum, and the anterior corpus callosum, and disorganized schizotypy correlated negatively with right cingulum, and superior and inferior longitudinal fasciculi. VBM analyses

showed a negative correlation of gray matter with negative schizotypy in the left cerebellum, while gyrification in the inferior parietal cortex correlated positively with negative (interpersonal) schizotypy. **Conclusions:** These findings pave the way for a neural network conceptualization of schizotypy as a psychosis proneness trait across the general population, showing associations with fronto-subcortical and frontotemporal systems as structural substrates of this risk phenotype.

Key words: cortical folding/gyrification/magnetic resonance imaging (MRI)/psychosis proneness

Introduction

Schizotypy is a human risk phenotype for the schizophrenia spectrum.^{1,2} It characterizes cognitive, emotional, and behavioral traits that are reminiscent of schizophrenia and associated with psychosis proneness, yet are prevalent across the general population including nonclinical subjects.³ Including positive, negative, and disorganized facets, schizotypy closely mirrors symptoms identified in psychotic disorders. Within the clinical schizophrenia spectrum, schizotypy has played a prominent role in defining spectrum disorders such as schizotypal personality disorder, which has shown neurobiological

similarities with schizophrenia⁴ including cognitive function⁵ and brain structural changes.^{6,7} Beyond the clinical spectrum, emerging from the identification of links between schizotypy in nonclinical populations and clinical cases (or those at risk) are recent neurobiological spectrum hypotheses that link neural systems across health, risk, and disease (review in ref. ²). These are consistent with “fully dimensional” models of schizotypy that might be extended to include nonclinical and clinical cohorts (for review see ref. ³).

Reliable identification of a neural signature or “bio-type” underlying schizotypy (or its single facets) would have considerable impact on both conceptualizing schizophrenia (and psychoses in general) as well as early identification of people at risk, since conventional clinical tools for early detection and intervention are either unspecific or capture phenomena immediately preceding the onset of psychosis.^{8–10}

Despite several initial studies, however, it has remained unclear which neural networks are associated with schizotypal traits. There are now several, mostly smaller studies that have used different self-assessment measures of schizotypal traits in nonclinical general population samples and related them to structural brain imaging correlates. The results are not unequivocal, identifying single regions associated with schizotypy, but these studies are mostly limited to regional volume analysis of gray matter. Some of this research has compared preselected extreme groups with high vs low schizotypy,^{11,12} while most others have used dimensional designs across a certain range of schizotypy, normally in the low to medium range of psychometric schizotypy, and thus below clinical thresholds for spectrum disorders.^{13–16} Not only have previous studies relied on smaller sample sizes (generally <100 participants). They have also typically focused on a single parameter characterizing brain structure, eg, regional brain volumes or white matter integrity. While there are now studies with larger cohorts analyzing regional volumes,¹⁷ there are hardly any studies analyzing the relation of schizotypy(-like) markers or psychotic-like experiences and gyrification or other cortical folding markers of early brain development.^{18,19} Hence, there is a significant need for adequately powered imaging studies of both white and gray matter in large nonclinical cohorts. Such analyses could close the gap in our understanding of the biological spectrum hypothesis, adding a brain network perspective. In particular, the paucity of structural connectivity studies^{12,16,20} has limited a network understanding of the biological bases of schizotypy.

From a network perspective, the previous findings on gray and white matter associations with schizotypy might be understood by focusing on networks rather than single brain regions. Given that schizophrenia itself is understood as a brain network disorder,²¹ analysis of brain structure in schizotypy might benefit from formulating hypothesis on the effects of schizotypy

(and its facets) on particular neural networks rather than single regions.²² Based on the existing body of evidence, 3 neural network hypotheses can be tentatively derived from the previous studies in psychiatrically healthy subjects. First, early studies have identified a potential link between schizotypy and default mode network (DMN) function, which is functionally altered in schizophrenia (for meta-analysis, see ref. ²³); this hypothesis is mostly based on structural studies linking the precuneus (a major DMN hub) to schizotypy, and is one of the few replicated findings in the field (mostly showing larger volumes in higher schizotypy).^{11,15,24} Second, several studies have identified correlations of psychometric schizotypal traits in healthy subjects with nodes of the fronto-thalamo-striatal system, including different lateral and medial prefrontal areas,^{12,14} parts of the striatum,²⁵ and thalamus²⁶—again mostly with positive schizotypy. This resonates with functional MR imaging studies showing prefrontal correlates of schizotypy,^{13,27,28} as well as pharmacological challenge studies of schizotypy and striatal dopamine release,²⁹ and surrogate markers of striatal dopamine function,³⁰ and striatal dopamine binding and prefrontal activation.³¹ Also, this hypothesis is of particular interest given the association of white matter tracts connecting prefrontal cortices with the thalamus (esp. the anterior limb of the internal capsule/anterior thalamic radiation) as well as interhemispheric corpus callosum fibers in the clinical spectrum of schizotypal personality disorder and schizophrenia.^{6,32} Finally, a third line of evidence, although from only a few studies, has suggested that aspects of frontotemporal connectivity, eg, integrity of the uncinate fasciculus and cingulum are linked to schizotypy^{12,33}; however, like individual studies implicating the hippocampus³⁴ or the interaction of fronto-striatal and cerebellar networks,³⁵ these findings have not widely been replicated so far.

Aiming to overcome some of the limitations of previous studies, we analyzed a large data set of almost 700 non-clinical subjects from the multi-center FOR2107 study.³⁶ Within these same subjects, we applied 3 different MRI method approaches to identify brain structural markers of schizotypy: (1) diffusion tensor imaging (DTI) as an indicator of white matter fiber tract integrity, (2) voxel-based morphometry (VBM), and (3) gyrification, which is a cortical folding biomarker that is temporally more stable than volume and an indicator of early (intrauterine and childhood) brain development. We specifically tested the competing hypotheses that schizotypy is linked to prefronto-thalamo-striatal brain structure (ie, gray matter of these regions as well as the integrity of interconnecting fiber tracts) vs the precuneus (as part of the DMN). The approach allows assessing several measures of brain structure and their association with different schizotypy facets on the phenotype level (ie, positive vs negative vs disorganized).

Table 1. Descriptive Statistics of Sample Demographics

Sex	Frequencies					
	251 male (37.3%)/422 female (62.7%)					
	Mean	SD (Standard Deviation)	Minimum	Maximum	Kurtosis	Skewness
Age	32.53	12.34	18	65	−0.294	1.001
IQ ^a	113.97	13.48	85	145	−0.689	0.480
SPQ-B total	3.33	3.01	0	16	1.279	1.156
SPQ-B Cognitive Perceptual	0.90	1.16	0	6	1.770	1.403
SPQ-B Interpersonal	1.67	1.70	0	8	0.720	1.091
SPQ-B Disorganized	0.76	1.25	0	6	2.994	1.875

^aEstimated with MWT-B (Mehrfachwahl-Wortschatztest-B⁷³).

Materials and Methods

Study Cohort

We included a cohort of $n = 673$ psychiatrically healthy subjects (422 women, 251 men; mean age 32.53 years, SD 12.34) from the general population, recruited as part of the FOR2107 study³⁶ in the cities of Marburg and Münster, Germany. Educational attainment, obtained based on the German secondary school and higher education (qualification) system, showed a high percentage of well-educated participants (9 years: 1.8%, 10 years: 9.5%, 12 years: 5.9%, 13 years: 49.5%, 15 years: 2.1%, 16 years [Bachelor's degree]: 13.7%, 18 years [Master's degree]: 17.4%).

The study protocol was approved by the local Ethics Committees of the Medical Schools of Philipps-Universität Marburg and Westfälische-Wilhelms-Universität Münster, respectively.

Subjects were recruited from the general population by advertisements and were compensated for participation (for details of the FOR2107 study, see ref. ³⁶). All subjects underwent a full clinical assessment using the German version of the Structured Clinical Interview for DSM-IV axis I diagnoses^{37,38} confirming (in addition to their self-report) the absence of a current or previous axis I psychiatric diagnosis. Further exclusion criteria included current or previous substance dependence, history of traumatic brain injury (with loss of consciousness), CNS pathologies, or uncontrolled general medical conditions. See [table 1](#) for further sample characteristics.

Phenotyping

We used the Schizotypal Personality Questionnaire-Brief version (SPQ-B) to assess subjects for schizotypy. The SPQ-B derives from the initial SPQ developed by Raine on the basis of DSM-III-R criteria for schizotypal personality disorder³⁹ and allows a dimensional assessment of the 3 major dimensions or facets of schizotypy: cognitive-perceptual (a positive symptom dimension), interpersonal (a negative symptom dimension), and

disorganized. Among its advantages for characterizing subjects' schizotypy levels is the widespread use and psychometric properties, similar to the extended version of the questionnaire.⁴⁰

The SPQ-B is based on a total of 22 items, which are assigned to the 3 dimensions SPQ-B-cognitive-perceptual (8 items), SPQ-B-interpersonal (8 items), and SPQ-B-disorganized (6 items). The established 3-factor structure of the SPQ-B and its origins from clinical criteria make it a compelling choice for a dimensional assessment of schizotypy aimed at targeting subphenotypes mirroring the common factor structure of clinical assessment tools. This factor structure is found in adolescents,^{41,42} undergraduate students,⁴³ as well as general healthy adult samples.⁴⁰ The SPQ-B thus allows robust assessment of schizotypy with its 3 main dimensions and comparability across a larger number of studies. Similar to previous studies, SPQ-B reliability (SPQ-B-total) was acceptable in both the total sample ($n = 673$; Cronbach's alpha 0.745) as well as in the DTI subsample ($n = 573$; Cronbach's alpha 0.724). See [table 1](#) for means and distribution of dimensional scores within the sample.

MRI Data Acquisition

T1-weighted structural MRI data were acquired at 3 Tesla scanners at the 2 sites in Marburg and Münster, respectively, using a harmonized multisite imaging protocol with ongoing quality assurance protocol including phantom scans.⁴⁴ At the Marburg site, MRI was obtained on a 3 T Siemens Tim Trio scanner (Siemens, Erlangen, Germany) with a 12-channel head matrix Rx-coil using a 3D MPRAGE sequence ($TR = 1.9$ s, $TE = 2.26$ ms, $TI = 900$ ms, flip angle = 7°) with 176 sagittal slices, 1 mm slice thickness, 256 mm field-of-view, and a resulting isotropic voxel resolution of $1 \times 1 \times 1$ mm³. At the Münster site, the 3D MPRAGE was obtained on a 3T Siemens Prisma system (Siemens, Erlangen, Germany) with a 20-channel head matrix Rx-coil and 192 slices and identical spatial resolution ($TR = 2.13$ s, $TE = 2.28$ ms, $TI = 900$ ms, flip angle = 8°).

DTI scans were acquired, at both centers, using isotropic diffusion-weighted images with an epi2d sequence as used in previous studies⁴⁵ ($TR = 7300$ ms, $TE = 90$ ms, $FOV = 320$ mm, phase encoding anterior-posterior; GRAPPA acceleration factor of 2, with 56 slices (2.5 mm slice thickness at the Münster site, 3 mm at Marburg site), 30 diffusion directions, and a final voxel resolution of $2.5 \times 2.5 \times 2.5$ mm³). Five non-diffusion-weighted images with $b = 0$ s/mm², and 2 sets of 30 diffusion-weighted images with $b = 1000$ s/mm² were acquired. For analyses, the 2 diffusion-weighted sets were merged. DTI images were visually inspected for artifacts and general data quality.

Imaging data from both centers were pooled based on extensive quality assurance protocols,⁴⁴ which included the regular scanning of phantoms.

MRI Data Preprocessing

We preprocessed DTI scans using tract-based analysis of diffusion parameters, and T1-weighted structural scans for VBM, surface-based morphometry analysis (SBM) of gyrification.

For analysis of DTI, we used FSL (version 5.02; FMRIB Software Library, FMRIB/Wellcome Centre of Integrative Neuroimaging, University of Oxford, United Kingdom^{46,47}) with an implemented pipeline for tract-based spatial statistics (TBSS) for group-level DTI analysis.^{48,49} Due to quality assurance, we excluded part of the initial sample for DTI analyses, leaving a total DTI subsample of $n = 573$ subjects (366 women/207 men; mean age 33.05 years, $SD = 12.57$). Diffusion-weighted images were corrected for motion and eddy current artifacts. Nonlinear registration into standard $1 \times 1 \times 1$ mm³ MNI-space (MNI-152) was achieved as part of TBSS using the FSL template. We calculated fractional anisotropy (FA) maps for each subject, which were projected onto the TBSS tract skeleton, as FA is the most commonly used DTI parameter in both studies of schizotypy¹² as well as the schizophrenia spectrum,^{6,50,51} thus allowing best comparability.

For preprocessing of T1-weighted scans, we used the VBM8 toolbox and CAT12 toolbox (build 1184, Christian Gaser, Structural Brain Mapping Group, Jena University Hospital, Jena, Germany). Both VBM8 and CAT12 are toolboxes implemented in the SPM software package (Statistical Parametric Mapping, Wellcome Centre For Human Neuroimaging, Institute of Neurology, London, United Kingdom), running on MatLab (The MathWorks, United States). The CAT12 toolbox includes a preprocessing pipeline SBM analyzes, which includes an analysis of gyrification based on the absolute mean curvature approach.

Images were first visually inspected for gross artifacts and malformations, and all images included in this analysis passed this initial quality check.

For VBM preprocessing, we used VBM8 default parameter sets, which included image segmentation into gray matter, white matter, and cerebrospinal fluid, as well as spatial normalization using the DARTEL algorithm. For smoothing, we applied a Gaussian kernel with 8 mm full-width at half maximum (FWHM). Preprocessing also included the calculation of total intracranial volume (TIV). VBM data were smoothed with an 8 mm FWHM Gaussian kernel.

For SBM preprocessing, we used the CAT12 toolbox's pipeline for extracting the cortical surface, followed by a calculation of the absolute mean curvature, from which our measure of gyrification is derived.⁵² Data were smoothed with a 20 mm FWHM kernel, given the spatial frequency of cortical folds, and in line with the CAT12 manual recommendations.

All T1-weighted images passed the CAT12 homogeneity check, which acts as a further quality assurance step in identifying outlier scans.

Statistical Analyses

We analyzed T1 morphometry data in SPM's general linear model framework using a multiple regression approach. In 4 separate models, we tested each of the 3 SPQ-B dimensions, as well as the SPQ-B total score, using a single (sub)score as regressor, as well as age and gender (in the case of VBM also TIV) as well as site (Marburg/Münster) and body coil (accounting for a change in body coil at the Marburg site during the course of the study) as nuisance variables, whose variance was removed. For correction of whole brain voxel-wise multiple comparisons, we applied family-wise error (FWE) cluster-level correction at $P < .05$ (following an initial peak-level threshold of $P < .001$, uncorr.). To be able to extract effect size measures, the resulting volume and surface T-maps were converted into Cohen's d maps using the CAT12 *transform* function.

For statistical analysis of DTI data, we used a tract-based region-of-interest approach, applying threshold-free cluster enhancement (TFCE) approach^{53,54} with 5000 permutations, and a $P < .05$ FWE-corrected threshold. To be able to extract effect size measures, the resulting T-maps were converted into d maps using *fslmaths*, Cohen's d at the peak voxel was then read out using *fslmeans*. Our DTI analysis included both testing of white matter tracts for which a specific anatomical hypothesis was formulated, ie, the anterior thalamic radiation forming the connection between (mediodorsal) thalamus and prefrontal cortex and thus the main core of the prefronto-thalamo-striatal circuit,⁵⁵ the uncinate fasciculus, and inferior fronto-occipital fasciculus, both implicated in one of the few previous DTI studies of schizotypal traits,¹² as well as other association tracts covered in the TBSS approach.

Results

DTI Findings

DTI analysis showed a number of significant correlations between SPQ-B scales and FA in white matter tracts.

While SPQ-B-cognitive-perceptual and SPQ-B-disorganized (as well as SPQ-B total) scores showed consistently negative correlations with FA across multiple white matter tracts (with effects sizes ranging from Cohen's $d = 0.039$ to $d = 0.168$ for SPQ-B-cognitive-perceptual, $d = 0.110$ to $d = 0.176$ for SPQ-B-disorganized, and $d = 0.117$ to $d = 0.215$ for SPQ-B total), the SPQ-B-interpersonal subscores showed positive correlations throughout (with effects sizes ranging between Cohen's $d = 0.145$ and $d = 0.187$).

A comprehensive overview of DTI findings is given in [table 2](#), with selected findings of interest in [figure 1](#).

Of note, correlations were found for the anterior thalamic radiation bilaterally (negative for the SPQ-B-cognitive perceptual dimension, but positive for the SPQ-B-interpersonal dimension), with a similar pattern for the anterior corpus callosum (forceps minor). In contrast, uncinate fasciculus FA was negatively correlated with SPQ-B-cognitive-perceptual subscores. Cingulum FA was associated with multiple dimensions, notably both cognitive-perceptual (bilateral, negative correlation) as well as interpersonal (left cingulum, positive correlation), disorganized (right cingulum, negative correlation), and total scores (right cingulum, negative correlation).

VBM Findings

VBM analysis showed a significant negative correlation of SPQ-B-interpersonal dimension with gray matter in a left superior cerebellar cluster ($P = 0.039$, FWE cluster-level corrected; $k = 808$; maximum intensity voxel at -27 ; -60 ; -26 with $d = 0.331$, Neuromorphometrics atlas), see [figure 2](#). A similar contralateral cluster was found in exploratory analysis ($P < 0.001$, uncorr.) in the right cerebellum ($k = 571$ voxels; maximum intensity voxel at 26 ; -56 ; -30 with $d = 0.302$), as well as the right precuneus ($n = 41$ voxels, maximum intensity voxel at 4 ; -44 ; 63 with $d = 0.262$), but none of these or other clusters reached either significance or trend-levels at FWE cluster-level corrections.

None of the other SPQ-B dimensions (or the SPQ-B total scores) showed significant correlations in VBM gray matter analyses.

Cortical Folding (Gyrification) Findings

Gyrification analyses showed a significant positive correlation ($P < 0.05$, FWE cluster-level corrected) of the SPQ-B-cognitive-perceptual dimension with a left inferior parietal cluster ($k = 610$ voxels, maximum intensity at -41 ; -54 ; 19 with $d = 0.330$), see [figure 3](#).

There were no other significant correlations (positive or negative) with other SPQ-B dimensions or the SPQ-B total scale.

Discussion

This study provides the first large-scale comprehensive gray and white matter morphometric analysis of schizotypal traits in a multi-center cohort of nonclinical subjects, testing their association to specific neural network models. We identify positive correlations for positive schizotypy and negative correlations for negative schizotypy within the anterior thalamic radiation, providing evidence for a differential association of nonclinical schizotypy with prefronto-subcortical connectivity. Gray matter showed negative correlations of negative schizotypy and cerebellar volumes, while the right precuneus failed to reach corrected significance levels. Gyrification only showed significant correlation between positive schizotypy and the left inferior parietal cortex. At the same time, findings also show associations with additional regions and networks depending on the facet of schizotypy. Hence, we shall discuss the main 3 aspects which this study contributes to advancing our understanding of how brain structural correlates of schizotypy and its facets relate to those of schizophrenia spectrum disorders.^{4,6}

Our findings provide some evidence for the prefronto-thalamo-striatal hypothesis laid out above, but fails to demonstrate consistent involvement of the precuneus or other DMN structures.

Some of the strongest single findings of this study are the white matter structural connectivity associations with both positive and negative schizotypy (albeit in different directions) with the anterior thalamic radiation, ie, the major tract carrying thalamo-frontal projections from the (mediodorsal) thalamus through the anterior limb of the internal capsule toward the prefrontal cortex,⁵⁵ and in addition the inferior fronto-occipital tract and the cingulum. These findings suggest that the connectivity of prefrontal areas both with the thalamus, but also temporal and occipital brain areas are correlated with variance in schizotypy scores. Connections between the prefrontal cortex and thalamus are organized through parallel circuits including the striatum,⁵⁶ where complex topologies seem to segregate the main functions of these loops.⁵⁷ Surprisingly, these findings are not matched by respective gray matter variations in the areas connected by these tracts, but only a singular cerebellar region. We interpret these findings as giving support to fronto-subcortical connectivity being at the core of both positive and negative schizotypy facets. Also, a recent review of structural and functional findings, which did not reveal consistent patterns related to overall schizotypy, has noted limitations related to methodological discrepancies between single studies (mostly of smaller sample size),²²

Table 2. Significant Correlations (TFCE, $P < .05$ FWE corrected) of SPQ-B Subscores and Total Score in $n = 573$ Healthy Subjects and Fractional Anisotropy (FA) Derived From TBSS Analysis of DTI Data

Tract	Cluster size k	P max	MNI-co-ordinates X Y Z	Cohen's d at Peak Voxel
1A: Negative correlations of SPQ-B cognitive-perceptual subscore and FA				
Left uncinate fasciculus	765	0.007	-24 16 15	0.1611
	25	0.044	-27 13 13	0.1509
Left superior longitudinal fasciculus	130	0.037	-50 -9 21	0.1488
Left superior longitudinal fasciculus (pars temporalis)	232	0.022	-50 -9 21	0.1488
Left inferior fronto-occipital fasciculus	550	0.015	-24 16 15	0.1611
Left anterior thalamic radiation	909	0.004	-24 16 15	0.1611
	19	0.046	-14 3 7	0.1207
	17	0.046	-11 6 1	0.1458
Left cingulum	977	0.006	-14 25 20	0.1296
	64	0.035	-15 -29 31	0.1680
Left corticospinal tract	649	0.019	-18 -21 57	0.1639
	473	0.032	-23 -14 12	0.1101
Right superior longitudinal fasciculus	3228	0.005	35 -25 35	0.1373
Right superior longitudinal fasciculus (pars temporalis)	1226	0.006	38 -9 26	0.1299
	121	0.028	39 -41 25	0.1300
	19	0.047	45 -40 21	0.1026
Right inferior longitudinal fasciculus	281	0.029	37 -22 -4	0.1337
	189	0.031	41 -35 -8	0.1198
	67	0.045	48 0 -17	0.0398
	43	0.047	46 -12 -8	0.0401
	23	0.049	47 -19 -2	0.0401
	20	0.049	50 -5 -11	0.0388
Right inferior fronto-occipitalis fasciculus	38	0.047	26 31 20	0.1562
Right anterior thalamic radiation	237	0.028	17 45 -9	0.1261
	218	0.008	27 30 20	0.1583
	111	0.028	20 51 7	0.1383
Right cingulum	44	0.026	17 -54 32	0.1246
Right cingulum (hippocampal part)	187	0.01	19 -48 19	0.1305
Right corticospinal tract	936	0.008	24 -9 14	0.1572
Forceps minor (corpus callosum, splenium)	3323	0.002	3 22 14	0.1400
1B: Positive correlations of SPQ-B interpersonal subscore and FA				
Left anterior thalamic radiation	422	0.004	-22 11 15	0.1746
Left cingulum	115	0.027	-10 21 19	0.1591
Right anterior thalamic radiation	52	0.029	20 14 9	0.1876
Right inferior fronto-occipitalis fasciculus	308	0.025	27 26 12	0.1537
Forceps minor (anterior corpus callosum)	113	0.019	14 21 22	0.1868
	98	0.04	-10 22 18	0.1448
1C: Negative correlations of SPQ-B disorganized subscore and FA				
Left inferior longitudinal fasciculus	219	0.021	-34 -60 23	0.1755
	28	0.041	-44 -23 -6	0.1563
Left superior longitudinal fasciculus	603	0.006	-34 -60 23	0.1755
	524	0.023	-29 -19 34	0.1096
	122	0.039	-51 -14 26	0.1364
Left superior longitudinal fasciculus (pars temporalis)	209	0.013	-39 -49 16	0.1422
	42	0.04	-51 -14 26	0.1364
	36	0.046	-34 -15 33	0.1157
	28	0.041	-52 -6 19	0.1202
	20	0.046	-38 -12 27	0.1141
1D: Negative correlations of SPQ-B total score and FA				
Left superior longitudinal fasciculus (pars temporalis)	16	0.042	-51 -10 22	0.1712
Right superior longitudinal fasciculus	549	0.023	34 -27 36	0.1388
	369	0.007	40 -42 21	0.2147
	71	0.032	58 -37 19	0.1666
Right superior longitudinal fasciculus (pars temporalis)	195	0.005	40 -43 20	0.2053
	40	0.038	34 -27 36	0.1388
Right inferior longitudinal fasciculus	544	0.023	42 -24 -1	0.1167
Right cingulum	106	0.003	17 -54 32	0.1472
Right cingulum (hippocampal part)	82	0.008	23 -53 29	0.1484

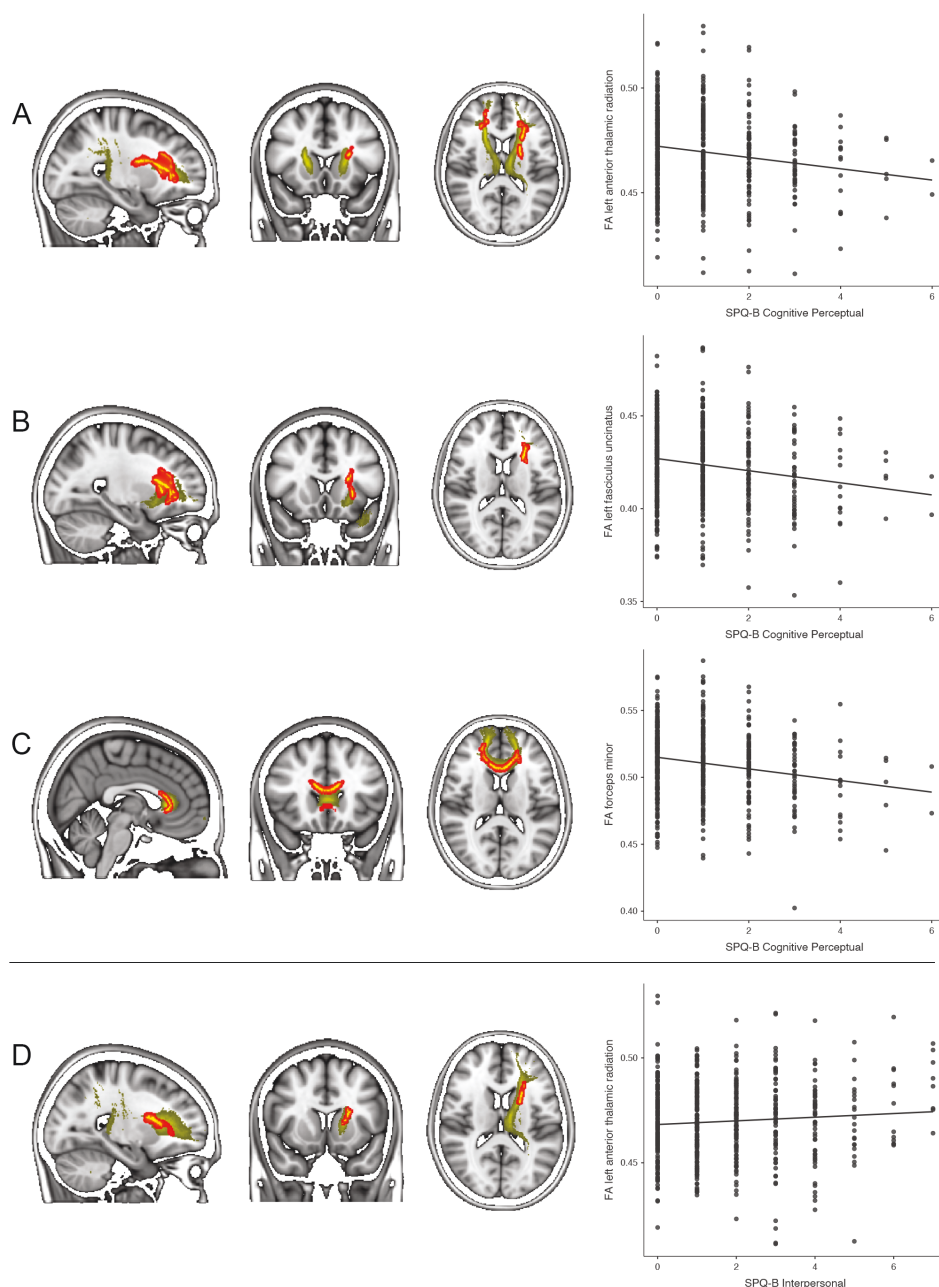


Fig. 1. Significant negative correlation (TFCE, $P < .05$ FWE corrected) of SPQ-B-cognitive-perceptual subscores with fractional anisotropy (FA) in (A) the (bilateral) anterior thalamic radiation, (B) uncinate fasciculus, and (C) anterior corpus callosum, as well as (D) SPQ-B-interpersonal subscores with FA in the anterior thalamic radiation.

which is mirrored in recent psychometric comparison studies of instruments.⁵⁸ Of note, recent findings from the ENIGMA consortium on gray matter associations with schizotypy did not identify significant correlations with subcortical structures, yet some cortical thickness variations were related to patterns observed in schizophrenia.¹⁷

This provides an important link to models of schizophrenia and the clinical spectrum,² where these areas show stronger structural reductions including white and gray matter.^{4,6,7,32} Interestingly our schizotypy findings in nonclinical subjects also mirror those of previous studies

in patients, where connectivity in some of these tracts like the anterior thalamic radiation and uncinate fasciculus are found to be correlated to symptom dimensions and clinical status.^{59,60} In contrast, our study did not find gray matter correlates in positive, negative, and disorganized schizotypy that would parallel either previous findings in nonclinical schizotypy^{11,14,15,24} or structural correlates of an analogous 3-factor structure in schizophrenia.⁶¹⁻⁶³ Reasons for this include the distribution of schizotypy traits in our sample, which was drawn from the general population and not specifically enriched to

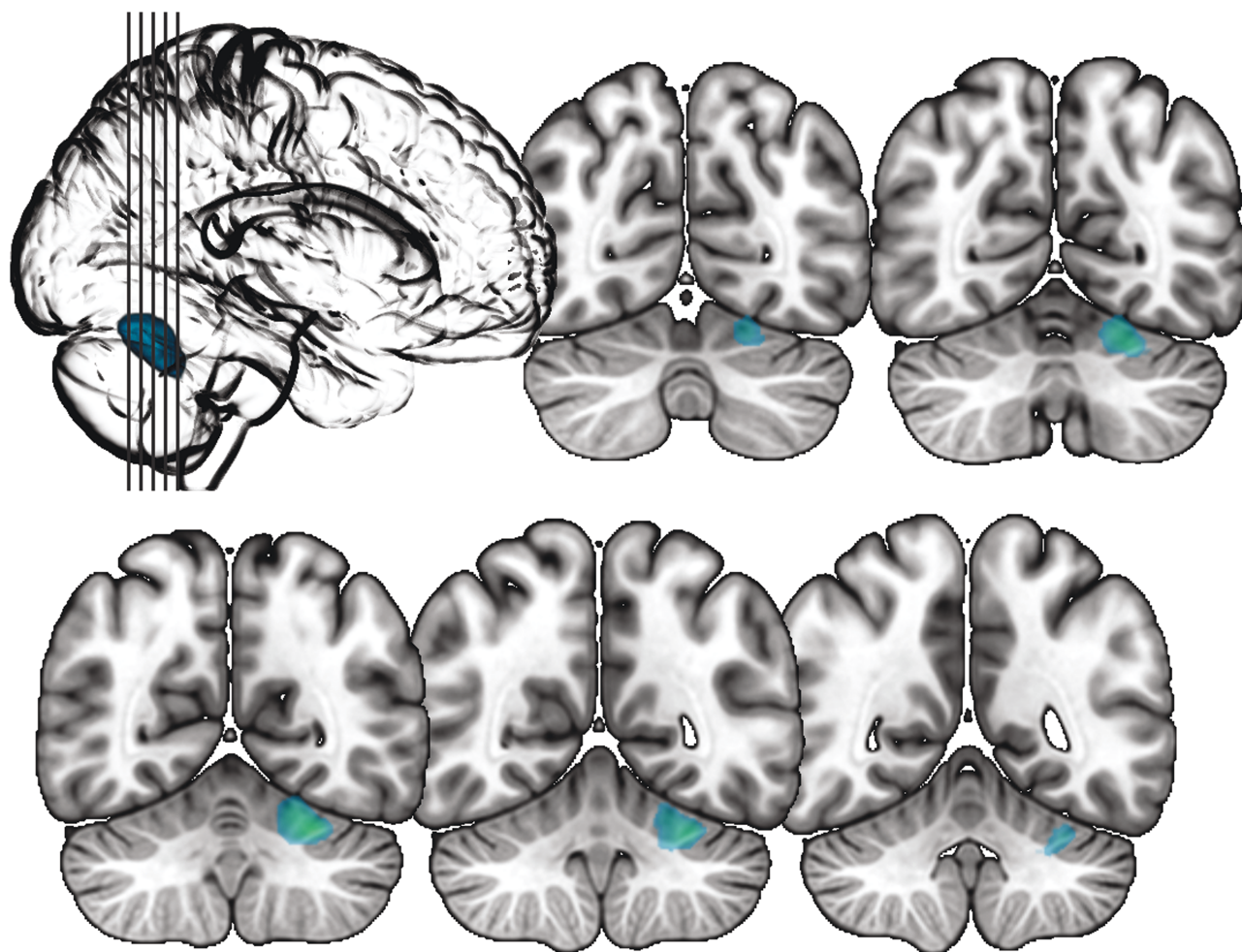


Fig. 2. Voxel-based morphometry (VBM) analysis of correlation of SPQ-interpersonal scores in $n = 673$ psychiatrically healthy subjects with gray matter, showing a significant ($P = .039$, FWE cluster-level corrected; $k = 808$ voxels) negative correlation in the left cerebellum (maximum intensity voxel at -27 ; -60 ; -26); note that for the purposes of display the image is given at $P < .001$ uncorr. threshold and $k = 800$ voxels extent threshold.

include “high-schizotypes” and thus had low to medium schizotypy scores, as well as schizotypy assessment tools and different effect sizes for white matter vs gray matter parameters. Still, it is remarkable that our cohort, in size similar to all previous nonclinical schizotypy morphometry studies combined, fails to show any fronto-subcortical gray matter associations. We suggest that previous VBM findings should therefore be interpreted cautiously and need further replication.

The lack of gyrification findings in the prefrontal cortex does not support the notion that subtle neurodevelopmental effects are associated with schizotypy—either overall or with single dimensions of the phenotype. It remains therefore unclear, whether and which aspects of schizotypy might be linked to hypothesized early developmental processes, as opposed to more fluctuating singular symptoms.⁶⁴ The association of negative schizotypy with gyrification of the inferior parietal cortex, an area relevant to multimodal integration and social cognition,⁶⁵ points to a potential relevance for

schizotypy and the psychosis spectrum; it has recently been linked to polygenic risk for schizophrenia,⁶⁶ but it is unclear whether this could provide a link to schizotypy.⁶⁷

Relevant parallels of prefrontal connectivity findings emerge with some recent resting-state fMRI studies. Functional connectivity in striatal and prefrontal seed regions was associated with positive (but not negative) dimension of schizotypy.²⁸ A similar effect for positive schizotypy was found when contrasting preselected high-schizotypes vs low-schizotypes and analyzing resting-state ventral prefrontal to ventral striatal connectivity.³⁵

In contrast, disorganized schizotypy shows associations with fiber tracts involved in speech and language, including divergent creative thinking which shows an opposite correlation in inferior longitudinal fasciculi.⁶⁸ This is consistent with the conceptualization of this symptom dimension in psychosis and the finding parallels associations with some of these tracts found in relation to disorganization symptoms in schizotypal personality disorder⁶⁹ and schizophrenia.⁷⁰

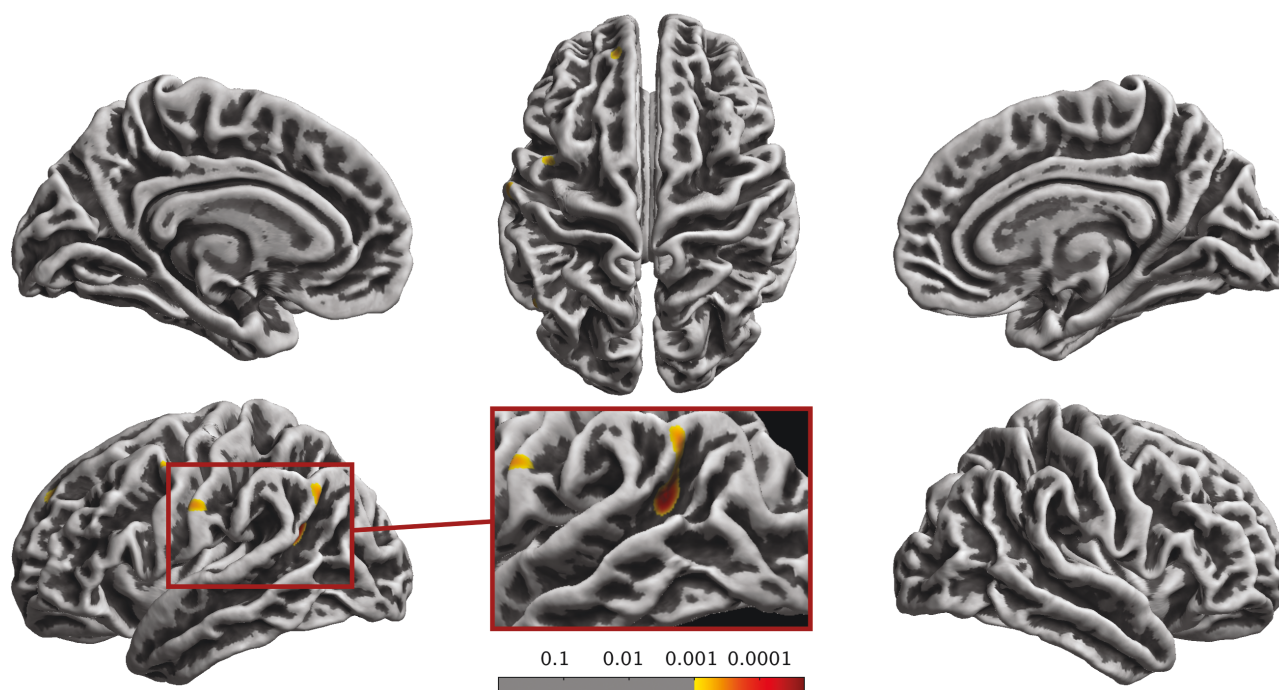


Fig. 3. Gyrification (absolute mean curvature method) analysis of correlation of SPQ-interpersonal scores in $n = 673$ psychiatrically healthy subjects with gray matter, showing significant ($P < 0.05$, FWE cluster-level corrected; $k = 610$ voxels) positive correlation. Note that for display purposes the image is given as $P < .001$ uncorr.

Hence, different connectivity patterns (including diametrically opposed associations as in the case of the anterior thalamic radiation) might in part be accounted for by different networks subserving different main aspects of schizotypy. A recent study of an alternative psychosis proneness/psychoticism phenotype⁷¹ has emphasized the interaction of DMN with an executive network (including lateral prefrontal areas), which can provide a framework for taking our network model to be tested in resting-state data.

While acknowledging the limitations of this study, including the rather low schizotypy scores in this unselected cohort, as well as the limitations of the particular schizotypy instrument used,⁴⁰ our findings provide strong support for structural connectivity markers (over those of regional volumes) to underlie nonclinical schizotypy. The prefronto-striatal system,⁷² which also provides close links to DMN and other relevant networks, seems to be at the core of both positive and negative schizotypy, while disorganized traits are related to frontotemporal connectivity. Our findings provide a dimensional (or spectrum) neural network model testable in structural and functional imaging studies and across the general population spectrum, which sets it apart from categorical models of psychiatric disorders.

Funding

Part of this work was supported by a FlexiFund grant of FCMH (to Igor Nenadić). This work is part of the

German multi-center consortium “Neurobiology of Affective Disorders. A translational perspective on brain structure and function,” funded by the German Research Foundation (Deutsche Forschungsgemeinschaft DFG; Forschungsgruppe/Research Unit FOR2107). Principal investigators (PIs) with respective areas of responsibility in the FOR2107 consortium are: Work Package WP1, FOR2107/MACS cohort, and brainimaging: Tilo Kircher (speaker FOR2107; DFG grant numbers KI 588/14-1 and KI 588/14-2), Udo Dannlowski (co-speaker FOR2107; DA 1151/5-1 and DA 1151/5-2), Axel Krug (KR 3822/5-1 and KR 3822/7-2), Igor Nenadic (NE 2254/1-2, NE 2254/2-1, NE2254/3-1, and NE2254/4-1), and Carsten Konrad (KO 4291/3-1). WP2, animal phenotyping: Markus Wöhr (WO 1732/4-1 and WO 1732/4-2), Rainer Schwarting (SCHW 559/14-1 and SCHW 559/14-2). WP3, miRNA: Gerhard Schratt (SCHR 1136/3-1 and 1136/3-2). WP4, immunology, and mitochondriae: Judith Alferink (AL 1145/5-2), Carsten Culmsee (CU 43/9-1 and CU 43/9-2), and Holger Garn (GA 545/5-1 and GA 545/7-2). WP5, genetics: Marcella Rietschel (RI 908/11-1 and RI 908/11-2), Markus Nöthen (NO 246/10-1 and NO 246/10-2), and Stephanie Witt (WI 3439/3-1 and WI 3439/3-2). WP6, multi-method data analytics: Andreas Jansen (JA 1890/7-1 and JA 1890/7-2), Tim Hahn (HA 7070/2-2), Bertram Müller-Myhsok (MU1315/8-2), and Astrid Dempfle (DE 1614/3-1 and DE 1614/3-2). CP1, biobank: Petra Pfefferle (PF 784/1-1 and PF 784/1-2), Harald Renz (RE 737/20-1 and 737/20-2).

CP2, administration. Tilo Kircher (KI 588/15-1 and KI 588/17-1), Udo Dannlowski (DA 1151/6-1), and Carsten Konrad (KO 4291/4-1). The study was supported by the German Federal Ministry of Education and Research (BMBF), through ERA-NET NEURON, “SynSchiz—Linking synaptic dysfunction to disease mechanisms in schizophrenia—a multilevel investigation” (01EW1810 to MR).

Acknowledgments and Members by Work Package (WP) WP1: Henrike Bröhl, Katharina Brosch, Bruno Dietsche, Rozbeh Elahi, Jennifer Engelen, Sabine Fischer, Jessica Heinen, Svenja Klingel, Felicitas Meier, Tina Meller, Torsten Sauder, Simon Schmitt, Frederike Stein, Annette Tittmar, and Dilara Yüksel (Dept. of Psychiatry, Marburg University). Mechthild Wallnig and Rita Werner (Core-Facility Brainimaging, Marburg University). Carmen Schade-Brittinger and Maik Hahmann (Coordinating Centre for Clinical Trials, Marburg). Michael Putzke (Psychiatric Hospital, Friedberg). Rolf Speier and Lutz Lenhard (Psychiatric Hospital, Haina). Birgit Köhnlein (Psychiatric Practice, Marburg). Peter Wulf, Jürgen Kleebach, and Achim Becker (Psychiatric Hospital Hephata, Schwalmstadt-Treysa). Ruth Bär (Care facility Bischoff, Neunkirchen). Matthias Müller, Michael Franz, Siegfried Scharmann, Anja Haag, Kristina Spenner, and Ulrich Ohlenschläger (Psychiatric Hospital Vitos, Marburg). Matthias Müller, Michael Franz, and Bernd Kundermann (Psychiatric Hospital Vitos, Gießen). Christian Bürger, Katharina Dohm, Fanni Dzvonyar, Verena Enneking, Stella Fingas, Katharina Förster, Janik Goltermann, Dominik Grotegerd, Hannah Lemke, Susanne Meinert, Nils Opel, Ronny Redlich, Jonathan Repple, Kordula Vorspohl, Bettina Walden, and Dario Zaremba (Dept. of Psychiatry, University of Münster). Harald Kugel, Jochen Bauer, Walter Heindel, and Birgit Vahrenkamp (Dept. of Clinical Radiology, University of Münster). Gereon Heuft and Gudrun Schneider (Dept. of Psychosomatics and Psychotherapy, University of Münster). Thomas Reker (LWL-Hospital Münster). Gisela Bartling (IPP Münster). Ulrike Buhlmann (Dept. of Clinical Psychology, University of Münster). WP2: Marco Bartz, Miriam Becker, Christine Blöcher, Annuska Berz, Moria Braun, Ingmar Conell, Debora dalla Vecchia, Darius Dietrich, Ezgi Esen, Sophia Estel, Jens Hensen, Ruhkshona Kayumova, Theresa Kisko, Rebekka Obermeier, Anika Pützer, Nivethini Sangarapillai, Özge Sungur, Clara Raithel, Tobias Redecker, Vanessa Sandermann, Finnja Schramm, Linda Tempel, Natalie Vermehren, Jakob Vörckel, Stephan Weingarten, Maria Willadsen, and Cüneyt Yildiz (Faculty of Psychology, Marburg University). WP4: Jana Freff, Silke Jörgens, and Kathrin Schwarte (Dept. of Psychiatry, University of Münster). Susanne Michels, Goutham Ganjam, and Katharina Elsässer (Faculty of Pharmacy, Marburg University). Felix Ruben Picard, Nicole Löwer, and Thomas Ruppertsberg (Institute of Laboratory Medicine

and Pathobiochemistry, Marburg University). WP5: Helene Dukal, Christine Hohmeyer, Lennard Stütz, Viola Schwerdt, Fabian Streit, Josef Frank, and Lea Sirignano (Dept. of Genetic Epidemiology, Central Institute of Mental Health, Medical Faculty Mannheim, Heidelberg University). WP6: Anastasia Benedyk, Miriam Bopp, Roman Keßler, Maximilian Lückel, Verena Schuster, and Christoph Vogelbacher (Dept. of Psychiatry, Marburg University). Jens Sommer and Olaf Steinsträter (Core-Facility Brainimaging, Marburg University). Thomas W. D. Möbius (Institute of Medical Informatics and Statistics, Kiel University). CP1: Julian Glandorf, Fabian Kormann, Arif Alkan, Fatana Wedi, Lea Henning, Alena Renker, Karina Schneider, Elisabeth Folwarczny, Dana Stenzel, Kai Wenk, Felix Picard, Alexandra Fischer, Sandra Blumenau, Beate Kleb, Doris Finholdt, Elisabeth Kinder, Tamara Wüst, Elvira Przepadlo, and Corinna Brehm (Comprehensive Biomaterial Bank Marburg, Marburg University).

Data Availability

All PIs take responsibility for the integrity of the respective study data and their components. All authors and coauthors had full access to all study data.

Conflicts of Interest

Biomedical financial interests or potential conflicts of interest: T.K. received unrestricted educational grants from Servier, Janssen, Recordati, Aristo, Otsuka, and neuraxpharm. Markus Wöhr is the scientific advisor of Avisoft Bioacoustics. The other authors have declared that there are no conflicts of interest in relation to the subject of this study.

Ethical Approval

The FOR2107 cohort project (WP1) was approved by the Ethics Committees of the Medical Faculties, University of Marburg (AZ: 07/14) and University of Münster (AZ: 2014-422-b-S).

References

1. Catts SV, Fox AM, Ward PB, McConaghy N. Schizotypy: phenotypic marker as risk factor. *Aust N Z J Psychiatry*. 2000;34:S101–S107.
2. Nelson MT, Seal ML, Pantelis C, Phillips LJ. Evidence of a dimensional relationship between schizotypy and schizophrenia: a systematic review. *Neurosci Biobehav Rev*. 2013;37:317–327.
3. Grant P, Green MJ, Mason OJ. Models of schizotypy: the importance of conceptual clarity. *Schizophr Bull*. 2018;44:S556–S563.

4. Siever LJ, Davis KL. The pathophysiology of schizophrenia disorders: perspectives from the spectrum. *Am J Psychiatry*. 2004;161:398–413.
5. Siddi S, Petretto DR, Preti A. Neuropsychological correlates of schizotypy: a systematic review and meta-analysis of cross-sectional studies. *Cogn Neuropsychiatry*. 2017;22:186–212.
6. Lener MS, Wong E, Tang CY, et al. White matter abnormalities in schizophrenia and schizotypal personality disorder. *Schizophr Bull*. 2015;41:300–310.
7. Hazlett EA, Goldstein KE, Kolaitis JC. A review of structural MRI and diffusion tensor imaging in schizotypal personality disorder. *Curr Psychiatry Rep*. 2012;14:70–78.
8. Schultze-Lutter F, Nenadic I, Grant P. Psychosis and schizophrenia-spectrum personality disorders require early detection on different symptom dimensions. *Front Psychiatry*. 2019;10:476.
9. van Os J, Linscott RJ, Myin-Germeys I, Delespaul P, Krabbendam L. A systematic review and meta-analysis of the psychosis continuum: evidence for a psychosis proneness-persistence-impairment model of psychotic disorder. *Psychol Med*. 2009;39:179–195.
10. Fusar-Poli P, Borgwardt S, Bechdolf A, et al. The psychosis high-risk state: a comprehensive state-of-the-art review. *JAMA Psychiatry*. 2013;70:107–120.
11. Modinos G, Mechelli A, Ormel J, Groenewold NA, Aleman A, McGuire PK. Schizotypy and brain structure: a voxel-based morphometry study. *Psychol Med*. 2010;40:1423–1431.
12. DeRosse P, Nitzburg GC, Ikuta T, Peters BD, Malhotra AK, Szeszko PR. Evidence from structural and diffusion tensor imaging for frontotemporal deficits in psychometric schizotypy. *Schizophr Bull*. 2015;41:104–114.
13. Aichert DS, Williams SC, Moller HJ, Kumari V, Ettinger U. Functional neural correlates of psychometric schizotypy: an fMRI study of antisaccades. *Psychophysiology*. 2012;49:345–356.
14. Ettinger U, Williams SC, Meisenzahl EM, Moller HJ, Kumari V, Koutsouleris N. Association between brain structure and psychometric schizotypy in healthy individuals. *World J Biol Psychiatry*. 2012;13:544–549.
15. Nenadic I, Lorenz C, Langbein K, et al. Brain structural correlates of schizotypy and psychosis proneness in a non-clinical healthy volunteer sample. *Schizophr Res*. 2015;168:37–43.
16. Pfarr JK, Nenadic I. A multimodal imaging study of brain structural correlates of schizotypy dimensions using the MSS. *Psychiatry Res Neuroimaging*. 2020;302:111104.
17. Kirschner M, Hodzic-Santor B, Antoniadis M, et al. Cortical and subcortical neuroanatomical signatures of schizotypy in 3004 individuals assessed in a worldwide ENIGMA study. *Mol Psychiatry*. 2022;27:1167–1176.
18. Meller T, Schmitt S, Ettinger U, et al. Brain structural correlates of schizotypal signs and subclinical schizophrenia nuclear symptoms in healthy individuals. *Psychol Med*. 2022;52:342–351.
19. Evermann U, Gaser C, Meller T, Pfarr JK, Grezelschak S, Nenadic I. Nonclinical psychotic-like experiences and schizotypy dimensions: associations with hippocampal subfield and amygdala volumes. *Hum Brain Mapp*. 2021;42:5075–5088.
20. Messaritaki E, Foley S, Barawi K, Ettinger U, Jones DK. Increased structural connectivity in high schizotypy. *Netw Neurosci*. 2023;7:213–233.
21. Brandl F, Avram M, Weise B, et al. Specific substantial dysconnectivity in schizophrenia: a transdiagnostic multimodal meta-analysis of resting-state functional and structural magnetic resonance imaging studies. *Biol Psychiatry*. 2019;85:573–583.
22. Tonini E, Quide Y, Kaur M, Whitford TJ, Green MJ. Structural and functional neural correlates of schizotypy: a systematic review. *Psychol Bull*. 2021;147:828–866.
23. Li S, Hu N, Zhang W, et al. Dysconnectivity of multiple brain networks in schizophrenia: a meta-analysis of resting-state functional connectivity. *Front Psychiatry*. 2019;10:482.
24. Modinos G, Egerton A, McLaughlin A, et al. Neuroanatomical changes in people with high schizotypy: relationship to glutamate levels. *Psychol Med*. 2018;48:1880–1889.
25. Meller T, Ettinger U, Grant P, Nenadic I. The association of striatal volume and positive schizotypy in healthy subjects: intelligence as a moderating factor. *Psychol Med*. 2019;50:2355–2363.
26. Di Carlo P, Pergola G, Antonucci LA, et al. Multivariate patterns of gray matter volume in thalamic nuclei are associated with positive schizotypy in healthy individuals. *Psychol Med*. 2019;50:1501–1509.
27. Premkumar P, Ettinger U, Inchley-Mort S, et al. Neural processing of social rejection: the role of schizotypal personality traits. *Hum Brain Mapp*. 2012;33:695–706.
28. Wang Y, Ettinger U, Meindl T, Chan RCK. Association of schizotypy with striatocortical functional connectivity and its asymmetry in healthy adults. *Hum Brain Mapp*. 2018;39:288–299.
29. Woodward ND, Cowan RL, Park S, et al. Correlation of individual differences in schizotypal personality traits with amphetamine-induced dopamine release in striatal and extrastriatal brain regions. *Am J Psychiatry*. 2011;168:418–426.
30. Rössler J, Unterassner L, Wyss T, et al. Schizotypal traits are linked to dopamine-induced striato-cortical decoupling: a randomized double-blind placebo-controlled study. *Schizophr Bull*. 2018;45:680–688.
31. Taurisano P, Romano R, Mancini M, et al. Prefronto-striatal physiology is associated with schizotypy and is modulated by a functional variant of DRD2. *Front Behav Neurosci*. 2014;8:235.
32. Hazlett EA, Collazo T, Zelmanova Y, et al. Anterior limb of the internal capsule in schizotypal personality disorder: fiber-tract counting, volume, and anisotropy. *Schizophr Res*. 2012;141:119–127.
33. Nelson MT, Seal ML, Phillips LJ, Merritt AH, Wilson R, Pantelis C. An investigation of the relationship between cortical connectivity and schizotypy in the general population. *J Nerv Ment Dis*. 2011;199:348–353.
34. Modinos G, Egerton A, McMullen K, et al. Increased resting perfusion of the hippocampus in high positive schizotypy: a pseudocontinuous arterial spin labeling study. *Hum Brain Mapp*. 2018;39:4055–4064.
35. Waltmann M, O'Daly O, Egerton A, et al. Multi-echo fMRI, resting-state connectivity, and high psychometric schizotypy. *Neuroimage Clin*. 2019;21:101603.
36. Kircher T, Wöhr M, Nenadic I, et al. Neurobiology of the major psychoses: a translational perspective on brain structure and function-the FOR2107 consortium. *Eur Arch Psychiatry Clin Neurosci*. 2019;269:949–962.
37. First MB, Gibbon M. The structured clinical interview for DSM-IV Axis I Disorders (SCID-I) and the Structured Clinical Interview for DSM-IV Axis II Disorders (SCID-II). *Comprehensive Handbook of Psychological Assessment, Vol. 2: Personality Assessment*. Hoboken, NJ: John Wiley & Sons Inc.; 2004:134–143.

38. Wittchen H-U, Wunderlich U, Gruschwitz S, Zaudig M. *SKID-I. Strukturiertes Klinisches Interview für DSM-IV*. Göttingen: Hogrefe; 1997.
39. Raine A. The SPQ: a scale for the assessment of schizotypal personality based on DSM-III-R criteria. *Schizophr Bull*. 1991;17:555–564.
40. Fonseca-Pedrero E, Ortuno-Sierra J, Lucas-Molina B, et al. Brief assessment of schizotypal traits: a multinational study. *Schizophr Res*. 2017;197:182–191.
41. Fonseca-Pedrero E, Paino-Pineiro M, Lemos-Giraldez S, Villazon-Garcia U, Muniz J. Validation of the schizotypal personality questionnaire-brief form in adolescents. *Schizophr Res*. 2009;111:53–60.
42. Ortuno-Sierra J, Badoud D, Knecht F, et al. Testing measurement invariance of the schizotypal personality questionnaire-brief scores across Spanish and Swiss adolescents. *PLoS One*. 2013;8:e82041.
43. Compton MT, Goulding SM, Bakeman R, McClure-Tone EB. An examination of the factorial structure of the Schizotypal Personality Questionnaire-Brief (SPQ-B) among undergraduate students. *Schizophr Res*. 2009;115:286–289.
44. Vogelbacher C, Mobius TWD, Sommer J, et al. The Marburg-Münster Affective Disorders Cohort Study (MACS): a quality assurance protocol for MR neuroimaging data. *Neuroimage*. 2018;172:450–460.
45. Pfarr JK, Brosch K, Meller T, et al. Brain structural connectivity, anhedonia, and phenotypes of major depressive disorder: a structural equation model approach. *Hum Brain Mapp*. 2021;42:5063–5074.
46. Jenkinson M, Beckmann CF, Behrens TE, Woolrich MW, Smith SM. FSL. *Neuroimage*. 2012;62:782–790.
47. Smith SM, Jenkinson M, Woolrich MW, et al. Advances in functional and structural MR image analysis and implementation as FSL. *Neuroimage*. 2004;23:S208–S219.
48. Smith SM, Jenkinson M, Johansen-Berg H, et al. Tract-based spatial statistics: voxelwise analysis of multi-subject diffusion data. *Neuroimage*. 2006;31:1487–1505.
49. Smith SM, Johansen-Berg H, Jenkinson M, et al. Acquisition and voxelwise analysis of multi-subject diffusion data with tract-based spatial statistics. *Nat Protoc*. 2007;2:499–503.
50. Vitolo E, Tatu MK, Pignolo C, et al. White matter and schizophrenia: a meta-analysis of voxel-based morphometry and diffusion tensor imaging studies. *Psychiatry Res Neuroimaging*. 2017;270:8–21.
51. Kelly S, Jahanshad N, Zalesky A, et al. Widespread white matter microstructural differences in schizophrenia across 4322 individuals: results from the ENIGMA Schizophrenia DTI Working Group. *Mol Psychiatry*. 2018;23:1261–1269.
52. Luders E, Thompson PM, Narr KL, Toga AW, Jancke L, Gaser C. A curvature-based approach to estimate local gyrification on the cortical surface. *Neuroimage*. 2006;29:1224–1230.
53. Smith SM, Nichols TE. Threshold-free cluster enhancement: addressing problems of smoothing, threshold dependence and localisation in cluster inference. *Neuroimage*. 2009;44:83–98.
54. Salimi-Khorshidi G, Smith SM, Nichols TE. Adjusting the effect of nonstationarity in cluster-based and TFCE inference. *Neuroimage*. 2011;54:2006–2019.
55. Axer H, Lippitz BE, von Keyserlingk DG. Morphological asymmetry in anterior limb of human internal capsule revealed by confocal laser and polarized light microscopy. *Psychiatry Res*. 1999;91:141–154.
56. Haber SN, Calzavara R. The cortico-basal ganglia integrative network: the role of the thalamus. *Brain Res Bull*. 2009;78:69–74.
57. Haber SN. Corticostriatal circuitry. *Dialogues Clin Neurosci*. 2016;18:7–21.
58. Pfarr JK, Meller T, Evermann U, Sahakyan L, Kwapil TR, Nenadic I. Trait schizotypy and the psychosis prodrome: current standard assessment of extended psychosis spectrum phenotypes. *Schizophr Res*. 2023;254:208–217.
59. Garver DL, Holcomb JA, Christensen JD. Compromised myelin integrity during psychosis with repair during remission in drug-responding schizophrenia. *Int J Neuropsychopharmacol*. 2008;11:49–61.
60. Serpa MH, Doshi J, Erus G, et al. State-dependent microstructural white matter changes in drug-naïve patients with first-episode psychosis. *Psychol Med*. 2017;47:2613–2627.
61. Koutsouleris N, Gaser C, Jager M, et al. Structural correlates of psychopathological symptom dimensions in schizophrenia: a voxel-based morphometric study. *Neuroimage*. 2008;39:1600–1612.
62. Nenadic I, Sauer H, Gaser C. Distinct pattern of brain structural deficits in subsyndromes of schizophrenia delineated by psychopathology. *Neuroimage*. 2010;49:1153–1160.
63. Zhang T, Koutsouleris N, Meisenzahl E, Davatzikos C. Heterogeneity of structural brain changes in subtypes of schizophrenia revealed using magnetic resonance imaging pattern analysis. *Schizophr Bull*. 2015;41:74–84.
64. Raine A. Schizotypal personality: neurodevelopmental and psychosocial trajectories. *Annu Rev Clin Psychol*. 2006;2:291–326.
65. Igelstrom KM, Graziano MSA. The inferior parietal lobule and temporoparietal junction: a network perspective. *Neuropsychologia*. 2017;105:70–83.
66. Liu B, Zhang X, Cui Y, et al. Polygenic risk for schizophrenia influences cortical gyrification in 2 independent general populations. *Schizophr Bull*. 2017;43:673–680.
67. Nenadic I, Meller T, Schmitt S, et al. Polygenic risk for schizophrenia and schizotypal traits in non-clinical subjects. *Psychol Med*. 2022;52:1069–1079.
68. Takeuchi H, Taki Y, Matsudaira I, et al. Convergent creative thinking performance is associated with white matter structures: evidence from a large sample study. *Neuroimage*. 2020;210:116577.
69. Chan CC, Szeszko PR, Wong E, et al. Frontal and temporal cortical volume, white matter tract integrity, and hemispheric asymmetry in schizotypal personality disorder. *Schizophr Res*. 2018;197:226–232.
70. Cavelti M, Winkelbeiner S, Federspiel A, et al. Formal thought disorder is related to aberrations in language-related white matter tracts in patients with schizophrenia. *Psychiatry Res Neuroimaging*. 2018;279:40–50.
71. Blain SD, Grazioplene RG, Ma Y, DeYoung CG. Toward a neural model of the openness-psychoticism dimension: functional connectivity in the default and frontoparietal control networks. *Schizophr Bull*. 2020;46:540–551.
72. Haber SN, Tang W, Choi EY, et al. Circuits, networks, and neuropsychiatric disease: transitioning from anatomy to imaging. *Biol Psychiatry*. 2020;87:318–327.
73. Lehrl S. *Mehrfachwahl-Wortschatz-Intelligenztest: MWT-B*. 5th ed. Göttingen: Testzentrale; 2005.